Journal of Applied Electrochemistry **34**: 935–943, 2004.

Electron transfer kinetics on boron-doped diamond Part I: Influence of anodic treatment

I. DUO[1], C. LEVY-CLEMENT[2], A. FUJISHIMA[3] and C. COMNINELLIS[1,*]
[1]*Ecole Polytechnique Fédérale de Lausanne, SB-ISP-UGEC, 1015 Lausanne, Switzerland*
[2]*LCMTR, CNRS,2-8 rue H. Dunant, 94320 Thiais, France*
[3]*Department of Applied Chemistry, School of Engineering, The University of Tokyo, Tokyo 113-8656, Japan*
*(*author for correspondence, fax: +41 21 693 3190, e-mail: christos.comninellis@epfl.ch)*

Received 22 April 2003; accepted in revised form 19 April 2004

Key words: anodic polarization, benzo/hydroquinone, boron-doped diamond electrodes, electron transfer reaction, ferri/ferrocyanide

Abstract

Boron-doped diamond electrodes, both as-grown and polarized anodically under different conditions, were prepared in order to study the chemical and electrochemical changes of diamond and clarify the role played by the surface-state density. Many different treatments were employed: as-grown (BDD_{ag}), mildly polarized (BDD_{mild}), strongly polarized in perchloric acid (BDD_{severe}), and strongly polarized in a sulphuric acid-acetic acid mixture (BDD_{AcOH}). Charge transfer processes at the electrode surface were studied by cyclic voltammetry. Simple electron transfer processes such as the outer-sphere redox system ferri/ferrocyanide ($Fe^{III/II}(CN)_6$) and complex charge transfer reactions such as the inner-sphere 1,4-benzoquinone/hydroquinone (Q/H_2 Q) redox reaction were chosen to test the electrochemical properties of the electrodes. The properties of the diamond electrodes were found to undergo strong modification as a function of surface treatment. The active surface area and the reaction rate constants decreased significantly upon anodic polarization. Important drops in the charge carrier concentration on the surface and in true surface area led to hindrance of electron transfer at the electrode.

1. Introduction

Among the factors that can influence the electrochemical behaviour of boron-doped diamond electrodes, the crystallographic structure [1, 2], the surface functional groups [3–5], the boron doping level [6, 7], and the presence of non-diamond amorphous carbon species (sp^2) [1, 8, 9] are probably the most important [10]. The preparation conditions and the surface treatment have a strong effect on the electrochemical behaviour of diamond electrodes [4, 11, 12]. Many kinds of surface treatment have been used so far, and the resulting changes in electrode properties have been investigated. Anodic polarization, oxygen plasma oxidation and boiling in strong acid are some of these surface treatment techniques [4, 5, 10–12]. Among the procedures employed, anodic oxidation is the simplest. The most evident result of anodic polarization is an improvement in reproducibility of the electrode response [13]. For this reason anodic oxidation has been widely used as a surface treatment for the electrochemical investigation of diamond electrodes. Significant changes in crystal morphology have not been found, but the chemical changes occurring on the surface during anodic polarization are still almost unknown. It was noticed that the background currents recorded in the potential window of electrolyte stability were higher at untreated diamond electrodes than at prepolarized ones [10], but no specific causes were identified to explain this feature. An important effect of the polarization appears to be the elimination of sp^2 species that can be more or less numerous on the diamond surface, depending on the preparation conditions. The importance of non-diamond species for electrode activity is not completely understood as yet. In the present work an attempt is made to clarify the influence of surface heterogeneity on the electronic properties of the diamond material, and particularly the importance of the sp^2 species in electron-transfer reactions.

2. Experimental details

Boron-doped diamond electrodes (BDD) were prepared by hot-filament chemical vapor deposition (HF-CVD) on p-type, low-resistivity (1–3 mΩ cm), {100} silicon wafers (Siltronix, diameter 10 cm, thickness 0.5 μm). The process gas was a mixture of 1% CH_4 in H_2 containing trimethylboron as a boron source (3 ppm, with respect to H_2). A gas flow of 5 $dm^3\,min^{-1}$ was

supplied into the chamber. Film growth occurred at a rate of 0.24 μm h^{-1}, and polycrystalline films were grown to a thickness of 1 μm with grain size from 200 to 800 nm. The boron/carbon ratio in the diamond films was about 3000 to 3500 ppm, corresponding to a concentration of 10^{20} to 10^{21} boron atoms cm^{-3} (the semiconductor-metal transition occurs at 2×10^{20} cm^{-3}).

As-grown boron-doped diamond electrodes (BDD_{ag}) were simply washed once with 2-propanol and twice with Milli-Q water in an ultrasonic bath in order to clean the surface without changing its hydrophobic properties. BDD electrodes polarized under mild conditions were obtained by 30 min of anodic polarization at 10 mA cm^{-2} of as-grown electrodes in 1 M H_2SO_4 (BDD_{mild}). BDD electrodes polarized under severe conditions were obtained by 576 h of anodic polarization at 1 A cm^{-2} of as-grown electrodes in 1 M $HClO_4$ at 40 °C (BDD_{severe}). Similar BDD electrodes polarized under severe conditions were also obtained by 16 h of anodic polarization at 1 A cm^{-2} of as-grown electrodes in 1 M H_2SO_4 + 3 M CH_3COOH (AcOH) at 40° C (BDD_{AcOH}).

The surface morphology was characterized by scanning electron microscopy (SEM) using a Jeol JMS-6300-F scanning electron microscope at up to 4000 times magnification. The BDD samples were analysed by X-ray photoelectron spectroscopy (XPS) in order to study the surface changes resulting from anodic treatments. The element analysis was carried out using a Kratos AXIS ULTRA system to calculate the O/C ratios on the sample surfaces after anodic treatments. A total area of 700 μm $\times$ 300 μm was analysed over a thickness of 50 ÷ 100 Å using a 15 kV Al-mono as the (monochromatic) X-ray source. Contact angles were measured by a Contact Angle Measuring System G10 (KRUSS, D).

A conventional three-electrode glass cell (0.1 L) was used for voltammetry. The counterelectrode was a platinum spiral. A Hg/Hg_2SO_4, K_2SO_4(sat) electrode was used as the reference electrode. All values of potential are reported relative to a standard hydrogen electrode (SHE). Cyclic voltammetry was performed with a computer-controlled Autolab PGstat30.

Solutions were prepare with Milli-Q water, reagents $K_4(FeCN)_6$, $K_3(FeCN)_6$, benzoquinone, hydroquinone, H_2SO_4 and $HClO_4$ were supplied by Fluka Chemie chemicals.

3. Results

3.1. *Morphological characterization*

SEM showed that the diamond morphology had not changed after mild polarization. In fact, diamond polarized under mild conditions (BDD_{mild}) exhibited exactly the same crystal morphology as that seen at as-grown (BDD_{ag}) diamond (Figure 1). After severe polarization (BDD_{severe} and BDD_{AcOH}), however, significant changes were visible. The colour of the surface had changed from blue to multicoloured (BDD_{severe}) or mirrorlike (BDD_{AcOH}). It was seen that after severe polarization (BDD_{severe} in Figure 1C) a diamond film was still present on the surface, but the morphology had

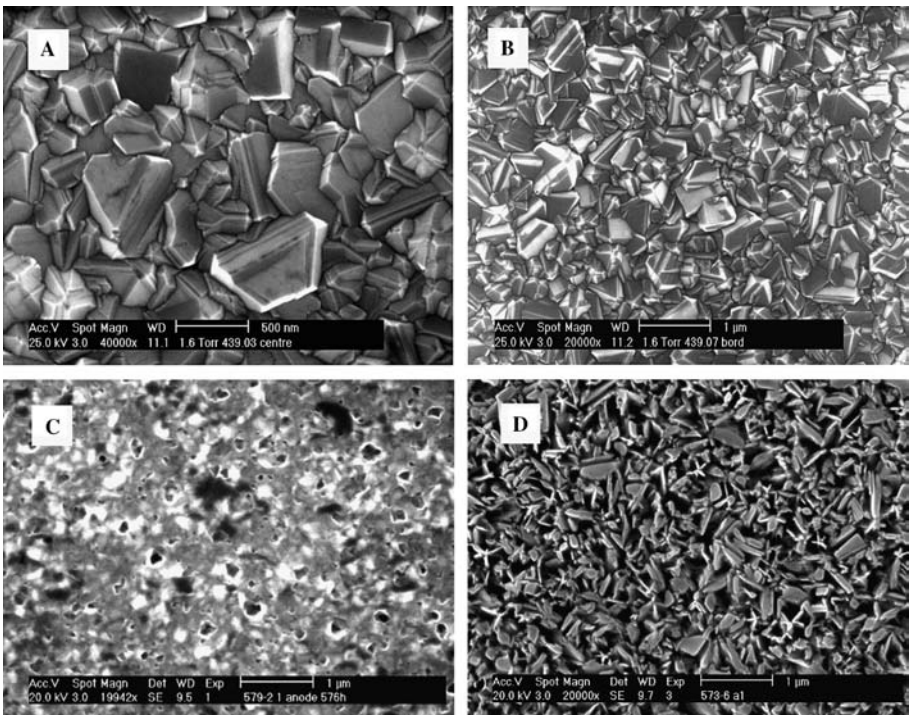

Fig. 1. SEM of BDD electrodes treated under differents conditions: (A) as-grown (BDD_{ag}); (B) after mild anodic polarization at 10 mA cm^{-2} in 1 M H_2SO_4 for 30 min; $T = 25$ °C (BDD_{mild}); (C) after severe anodic polarization at 1 A cm^{-2} in 1 M $HClO_4$ for 576 h; $T = 40$ °C (BDD_{severe}); (D) after anodic polarization at 1 A cm^{-2} in 1 M H_2SO_4 + 3 M CH_3COOH for 16 h; $T = 40$ °C (BDD_{AcOH}).

Table 1. Oxygen/carbon ratios and water contact angles found at BDD electrodes after different treatments

Electrode	Oxygen/Carbon	Contact angle/deg.
BDD_{ag}	0.08	102.5
BDD_{mild}	0.22	57
BDD_{severe}	0.26	53
BDD_{AcOH}	2.74	76

completely changed: the polycrystalline structure of diamond was no longer visible. After severe treatment in the presence of acetic acid (BDD_{AcOH}), the crystal edges were smoother, and a strong change in crystal shape and size had occurred as the typical result of a polishing process (Figure 1D).

Contact angle and XPS measurements were performed at all electrodes prepared in order to quantify the wettability of the samples and correlate it with the oxygen/carbon surface ratio (atomic %). Table 1 shows results for the oxygen/carbon ratio and the contact angles found after different treatments. Mild anodic polarization (BDD_{mild}) led to an increase in the oxygen/carbon ratio due to the introduction of oxygen-terminated functional groups on the diamond surface. Contact angle measurements were also made to characterize the solid/water interactions. Water on an as-grown diamond (BDD_{ag}) had a contact angle higher than 90°, typical of a nonwettable material. Oxygen introduced by anodic polarization and/or elimination of adsorbed hydrogen increased the wettability of the surface, as shown by the decrease of the contact angle of water from BDD_{ag} to BDD_{mild}. The contact angle did not change significantly when going from BDD_{mild} to a strong polarized diamond (BDD_{severe}). Because of the relation between wettability and oxygen coverage, it can be deduced that after mild polarization, the surface was completely oxidized and severe polarization treatment (BDD_{severe}) did not further increase the oxygen level. Quite different behaviour was seen at BDD_{AcOH} : the O/C ratio increased by one order of magnitude. The strong decrease in the carbon signal relative to the oxygen peak indicated a strong change in surface composition and morphology of the samples. The higher contact angle, in fact, indicated a higher degree of smoothness typical of a polished surface.

3.2. *Surface redox processes on BDD surfaces*

The electrochemical response of the electrodes varied as a function of surface treatment (Figure 2). Untreated electrodes (BDD_{ag}) exhibited the highest surface activity. The voltammogram revealed many surface redox transitions represented by overlapping current waves in the voltammetric curve (Figure 2). The electrode response decreased significantly after mild anodic polarization. In fact, the voltammetric response of BDD_{mild} electrodes revealed a decrease in surface activity, and only one well-defined irreversible pair of peaks was still visible (Inset in Figure 2), probably attribuable to surface redox functions. The peak current decreased and the irreversibility of the surface redox couple increased with increasing severity of the treatment (BDD_{severe}). The lowest activity was recorded after the treatment in the presence of AcOH (BDD_{AcOH}) (Inset in Figure 2).

Cyclic voltammograms were recorded for all electrodes at different scan rates (not given). The current did

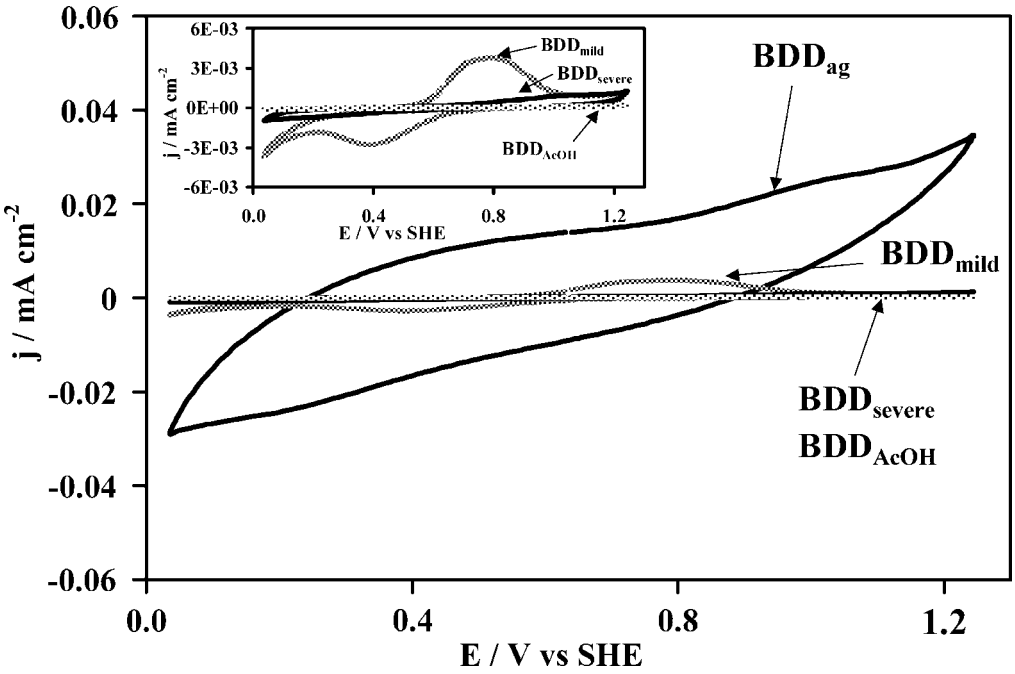

Fig. 2. Cyclic voltammograms of BDD electrodes in 0.5 M H_2SO_4. Scan rate 0.05 V s^{-1}; $T = 25$ °C. Inset: Zoom of Figure 2. for BDD_{mild}, BDD_{severe} and BDD_{AcOH}.

Table 2. Voltammetric charge, Q, and active surface ratio for BDD electrodes after different treatments

Electrode	5 mV s^{-1}		10 mV s^{-1}		20 mV s^{-1}		50 mV s^{-1}	
	Q /mC cm^{-2}	Q/Q_{AcOH}	Q /mC cm^{-2}	Q/Q_{AcOH}	Q /mC cm^{-2}	Q/Q_{AcOH}	Q /mC cm^{-2}	Q/Q_{AcOH}
BDD_{ag}	1.5	238	9.1×10^{-1}	236	5.6×10^{-1}	222	3.7×10^{-1}	244
BDD_{mild}	1.2×10^{-1}	19	7.3×10^{-2}	19	4.8×10^{-2}	19	3.2×10^{-2}	21
BDD_{severe}	4.7×10^{-2}	6	2.4×10^{-2}	6	1.8×10^{-2}	7	9.3×10^{-3}	6
BDD_{AcOH}	6.3×10^{-3}	1	3.8×10^{-3}	1	2.5×10^{-3}	1	1.5×10^{-3}	1

Values refer to the electrode geometric surface area of 1 cm^2; Electrolyte: 0.5 M H_2SO_4; T = 25 °C.

Table 3. Capacitance values calculated by cyclic voltammetry at different potential values (V vs SHE) after treatment of the diamond surface

Electrode	Capacitance/μF cm^{-2}					
	5×10^{-3} V s^{-1}			5×10^{-2} V s^{-1}		
	0.64 V	0.8 V	1.1 V	0.64 V	0.8 V	1.1 V
BDD_{ag}	749	497	180	231	206	100
BDD_{mild}	117	55	43	22	38	10
BDD_{severe}	7	10	11	3	4	7
BDD_{AcOH}	2	2.6	2	1	0.8	0.7

Investigations at two different scan rates: 5 and 50 mV s^{-1}; geometric surface area: 1 cm^2; electrolyte: 0.5 M H_2SO_4; T = 25 °C.

not increase as a linear function of scan rate, indicating the presence of irreversible redox surface processes [14]. From the measurements, the voltammetric charge (Q) was calculated at different scan rates as the integral of the anodic part of the voltammogram. The values of charge, which are a measure of surface activity of the electrodes, are shown in Table 2. If the voltammetric charge of BDD_{AcOH} electrodes is assumed to represent the activity of a totally clean diamond surface, then charge values normalized to the charge of BDD_{AcOH} ($Q_x Q_{AcOH}$) will provide a measure of active surface area of the electrodes. This ratio attains values higher than 200 for the BDD_{ag} electrodes (Table 2). This is due to the presence of functional groups electrochemically active on the electrode surface. A first treatment would eliminate part of these surface groups while reducing the surface activity (BDD_{mild}). A further, severe treatment then reduces the electrode activity (BDD_{severe} and BDD_{AcOH}) very significantly.

By cyclic voltammetry, the double-layer capacitance, C_{dl} can also be estimated using Equation 1. Values of double-layer capacitance calculated via the total (anodic and cathodic) currents, i, as functions of the scan rate, v, are shown in Table 3 for different applied potentials. These values refer to the electrode geometric surface area (1 cm^2).

$$i = 2C_{dl}v \quad (1)$$

The capacitance values vary with potential because of the presence of surface redox systems active at different potentials. Following severe treatment of the electrodes the capacitance values decreased significantly, and became almost potential independent. After anodic polarization (BDD_{mild}) the calculated capacitance was one order of magnitude lower than for fresh electrodes (BDD_{ag}). Severe polarization processes led to a further capacitance decrease at the interface (BDD_{severe} and BDD_{AcOH}).

3.3. *Electrochemical behaviour of soluble redox systems at BDD electrodes*

The electrochemical properties of diamond electrodes towards redox systems in the solution are sensitive to prior surface treatments. Two redox systems were studied at diamond electrodes in an attempt to correlate the electrochemical response of the electrodes with the surface treatment.

3.3.1. *Outer-sphere electron transfer reactions*

The outer-sphere ferri/ferrocyanide ($Fe^{III/II}(CN)_6$) couple is a simple one-electron transfer process, yet its behaviour is strongly influenced by the nature of the electrode surface. Cyclic voltammetry in presence of this redox system was performed on BDD electrodes after their anodic oxidation so as to elucidate the relation between electrochemical activity and chemical nature of the diamond electrode surface. The cathodic and anodic transfer coefficients (α_{red} and β_{ox} respectively), the apparent potential, $E^{\circ\prime}_{app}$ (defined as the experimental equilibrium potential of the redox couple in solution [15]), and the electrochemical rate constant k° were calculated. Considering the highly metallic character of boron-doped diamond electrodes (10^{20} to 10^{21} boron atoms cm^{-3}), equations developed for metal electrodes were

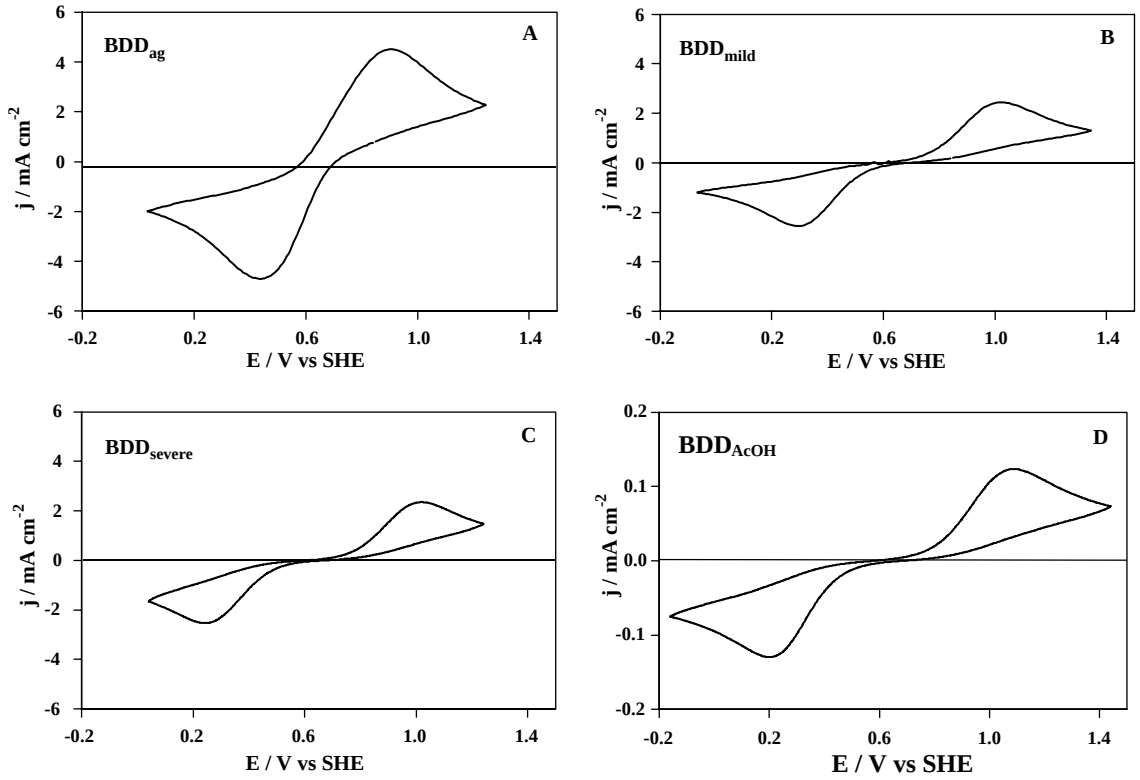

Fig. 3. Cyclic voltammograms of the redox couple $Fe^{III/II}(CN)_6$ $12.5 \times 10^{-3}/12.5 \times 10^{-3}$ M in 0.5 M H_2SO_4. Scan rate 0.1 V s^{-1}; $T = 25$ °C. (A) BDD_{ag}, (B) BDD_{mild}, (C) BDD_{severe}, (D) BDD_{AcOH}.

used for the mathematical treatment of experimental results (Equations 2–4) for irreversible reactions. Thus,

$$i_p = \left(2.99 \times 10^5\right)\alpha^{1/2} A C_0 D_0^{1/2} v^{1/2} (n = 1) \qquad (2)$$

The voltammetric response of the electrodes changed with the surface treatment, as shown in Figure 3. The largest currents were recorded at BDD_{ag} electrodes. At polarized electrodes (BDD_{mild} and BDD_{severe}), the peak currents were only half as large. A very low response (ten times lower) was obtained at BDD_{AcOH} electrodes.

The redox behaviour was tested at different scan rates at the four BDD electrodes (not given) in order to calculate the kinetic parameters of the reaction. The redox system was irreversible at all BDD electrodes ($\Delta E_p > 59$ mV for 1 electron). Both oxidation and reduction peaks exhibited the typical trend of irreversible systems following the equation that relates the peak potentials, E_p and the half-peak potential, $E_{p/2}$ (Equation 3):

$$\left|E_p - E_{p/2}\right| = 1.857\frac{RT}{\alpha F} = \frac{47.7}{\alpha} \quad \text{(method 1)} \qquad (3)$$

where potentials are in mV at 25 °C.

From Equation 3, the transfer coefficients α_{red} (cathodic reaction) and β_{ox} (anodic reaction) were calculated (method 1). Because of the dependence of the peak potentials on scan rate, the transfer coefficients were also calculated using the following equation (method 2):

$$E_p = E^\circ + \frac{RT}{\alpha nF}\left(0.78 - \ln k^\circ + \ln\sqrt{D^\circ \frac{\alpha nF}{RT}}\right) - \frac{RT}{2\alpha F}\ln v \quad \text{(method 2)} \qquad (4)$$

Table 4. Parameters of the redox system $Fe^{III/II}(CN)_6$ $12.5 \times 10^{-3}/12.5 \times 10^{-3}$ M calculated from the results of cyclic voltammetry performed at different diamond electrodes

Electrode	ΔE_p /V	$E^{\circ'}_{app}$ /V vs SHE	β_{ox} (1)	β_{ox} (1)	α_{red} (2)	α_{red} (2)	k^* /cm s^{-1}	k^{**} /cm s^{-1}	k° /cm s^{-1}
BDD_{ag}	0.24	0.67	0.3	0.3	0.4	0.3	3×10^{-4}	4×10^{-4}	4×10^{-4}
BDD_{mild}	0.53	0.66	0.3	0.3	0.3	0.3	1×10^{-4}	6×10^{-5}	8×10^{-5}
BDD_{severe}	0.52	0.63	0.3	0.3	0.3	0.3	8×10^{-5}	9×10^{-5}	9×10^{-5}
BDD_{AcOH}	0.62	0.64	0.2	0.3	0.3	0.3	4×10^{-5}	1×10^{-5}	2×10^{-5}

Electrolyte: 0.5 M H_2SO_4; $T = 25$ °C.
(1) determined from Equation 3, $k^* = k^\circ$ determined from the oxidation peak, $k^\circ = (k^* + k^{**})/2$.
(2) determined from Equation. 4, $k^{**} = k^\circ$ determined from the reduction peak.

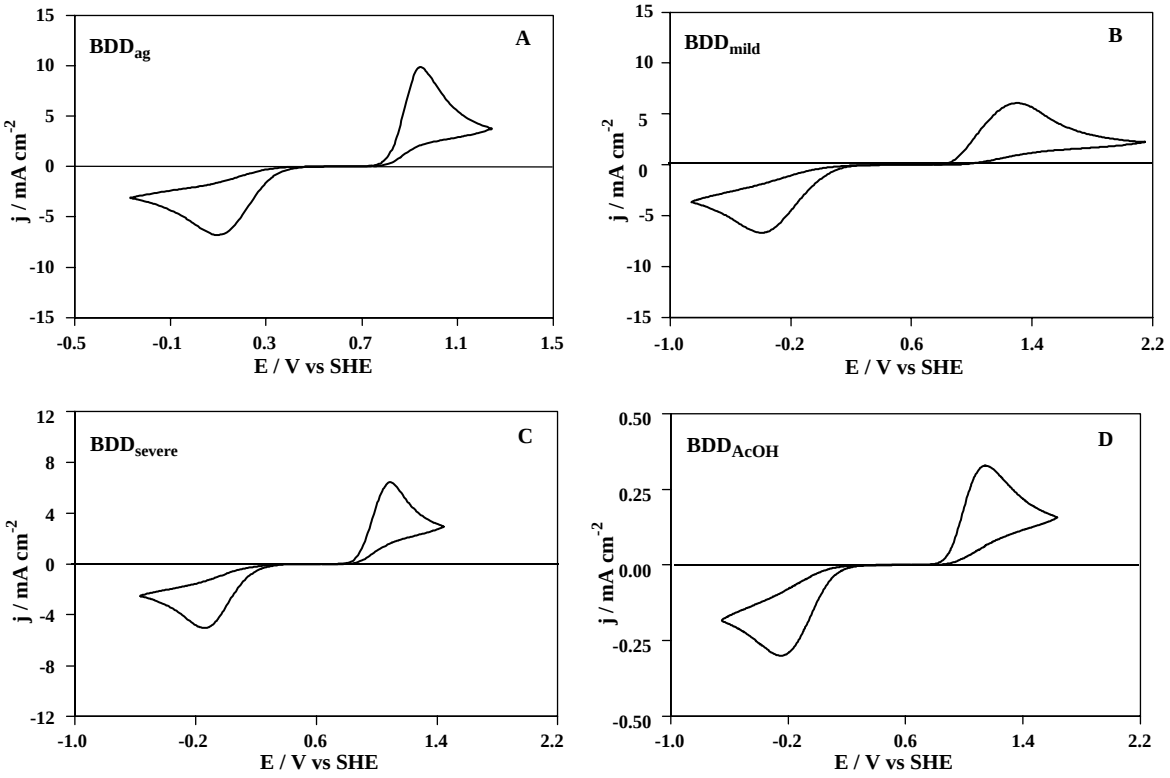

Fig. 4. Cyclic voltammograms of the redox couple Q/H_2Q $12.5 \times 10^{-3}/12.5 \times 10^{-3}$ M in 0.5 M H_2SO_4. Scan rate 0.1 V s^{-1}; $T = 25$ °C. (A) BDD_{ag}, (B) BDD_{mild}, (C) BDD_{severe}, (D) BDD_{AcOH}.

The results were compared with those obtained with method 1 (Equation 3). The reaction rate constants, k° were also calculated with Equation 4 while allowing for literature values of the diffusion coefficient, D° (7.35×10^{-6} cm^2 s^{-1} for $Fe^{II}(CN)_6$ and 6.7×10^{-6} cm^2 s^{-1} for $Fe^{III}(CN)_6$ [16]), one electron being involved in the electron transfer process. Such a mathematical treatment was applied to the results from all electrodes investigated. Table 4 summarizes the calculated parameter values. The as-grown diamond had a high activity toward the redox couple, whereas the same electrode was deactivated after anodic polarization. The reaction became more irreversible as indicated by the ΔE_p increase with the polarization. The shift of the apparent equilibrium potential, $E^{o\prime}_{app}$ with the treatment indicates a non symmetrical behaviour, typical of a semiconductor character of the material. The current peaks decreased significantly after oxidation of the electrode surface, indicating deactivation. The transfer coefficients, α_{red} and β_{ox}, were not so sensitive to the anodic treatment. The sum of the transfer coefficients did not add up to unity (as it should according to theory for metallic materials) at any of the diamond electrodes investigated. The values calculated for the reaction rate constant on BDD_{ag} electrodes were consistent with those reported [17, 18]. The reaction rate constant values could be compared as all tested electrodes had similar transfer coefficients, α_{red} and β_{ox}. For treated diamond electrodes, the values decreased by one order of magnitude relative to those found at BDD_{ag}. The low values of k° were due to a slow electron transfer process.

3.3.2. *Inner-sphere electron transfer reactions*

The behaviour of the inner-sphere benzoquinone/hydroquinone redox system was investigated on BDD electrodes as an example of a more complex redox reaction.

Table 5. Parameters of the redox system Q/H_2Q $12.5 \times 10^{-3}/12.5 \times 10^{-3}$ M calculated from the results of cyclic voltammetry performed at different diamond electrodes

Electrode	ΔE_p /V	$E^{o\prime}_{app}$ /V vs SHE	β_{ox} (1)	β_{ox} (1)	α_{red} (2)	α_{red} (2)	k^* /cm s^{-1}	k^{**} /cm s^{-1}	k° /cm s^{-1}
BDD_{ag}	0.74	0.52	0.5	0.3	0.3	0.3	9.7×10^{-5}	4.1×10^{-5}	7×10^{-5}
BDD_{mild}	1.42	0.45	0.2	0.2	0.2	0.2	2.1×10^{-5}	2.6×10^{-5}	2×10^{-5}
BDD_{severe}	0.93	0.48	0.3	0.3	0.3	0.2	8.3×10^{-6}	5.1×10^{-5}	6×10^{-5}
BDD_{AcOH}	1.18	0.46	0.3	0.3	0.2	0.3	4.2×10^{-7}	2.5×10^{-6}	1×10^{-6}

Electrolyte: 0.5 M H_2SO_4; $T = 25$ °C.
(1) determined from Equation 3 $k^* = k^\circ$ determined from the oxidation peak $k^\circ = (k^* + k^{**})/2$.
(2) determined from Equation 4 $k^{**} = k^\circ$ determined from the reduction peak.

This redox system was particularly interesting because of the complexity of the aromatic molecular structure and because of a multistep process involving the consecutive transfer of two electrons and two protons. Cyclic voltammetry was performed at the different diamond electrodes (Figure 4). Voltammetry was also performed at different scan rates in order to evaluate the kinetic parameters of the reaction (not given). The mathematical treatment used was that for metal electrodes (Equations 2–4). Values of $D^{\circ} = 8.5 \times 10^{-6}$ $cm^2\,s^{-1}$ and $9.8 \times 10^{-6}\,cm^2\,s^{-1}$ were used for the diffusion coefficients of hydroquinone and benzoquinone, respectively [19]. Table 5 shows the calculated parameter values.

The reaction was slow on all diamond electrodes investigated. A first observation was an increase in irreversibility (estimated from the ΔE_p) of the redox couple from BDD_{ag} to BDD_{AcOH}. An important factor was the more important sensitivity of the cathodic part of the voltammograms to the surface treatment, shown by the shift of the apparent equilibrium potential, $E^{\circ\prime}_{app}$ The $\alpha + \beta$ values found for the diamond electrodes were lower than unity and the rate constants, k° were different for the oxidation and reduction reactions on account of the semiconductor character of the boron-doped diamond material. The reaction rate constant values could be compared as all tested electrodes had similar transfer coefficients, α_{red} and β_{ox}. The values of the rate constant decreased with increasing severity of the treatment. The lower response seen at electrodes after a polishing-like process (BDD_{AcOH}) was probably due to the corresponding changes in crystal size and shape, as found with the ferri/ferrocyanide system.

Discussion

A decrease in surface activity following surface treatment had been observed. In the case of BDD_{ag} and BDD_{mild} electrodes (Table 3), the high capacitance values contain contributions of a true double-layer capacitance and of a pseudocapacitance associated with surface redox systems. The very low capacitance values obtained for strongly treated BDD electrodes indicate that surface redox transitions were eliminated from the diamond surface, and only a double-layer capacitance due to the charge distribution at the electrode–electrolyte interface can be calculated. In many papers a modification of the charge carrier concentration at the diamond surface was suggested as a result of the treatment [10, 17, 18, 20–22]. Other groups suggested that surface hydrogen or oxygen terminations may be responsible for the surface activity [4, 5, 12, 23]. The nature of the charge carriers has not been unambiguously defined so far. To explain the BDD behaviour, a non-negligible amount of sp^2 species may be assumed to be present in the grain boundaries of fresh electrodes (BDD_{ag}) [1, 8, 9]. In fact, redox equilibria could exist and generate such a high electrode activity, only in the presence of unsaturated carbon bonds on the diamond surface. By analogy with glassy carbon and graphite electrodes [14, 24, 25], the typically aromatic basic structure of non-diamond carbon could be responsible for the high surface activity of BDD_{ag} electrodes. It is well known that carbon-based electrodes have a six-membered ring structure in which benzoquinone/hydroquinone and carboxyl-like functional groups are present [26] (Figure 5). Anodic polarization led to oxidation of

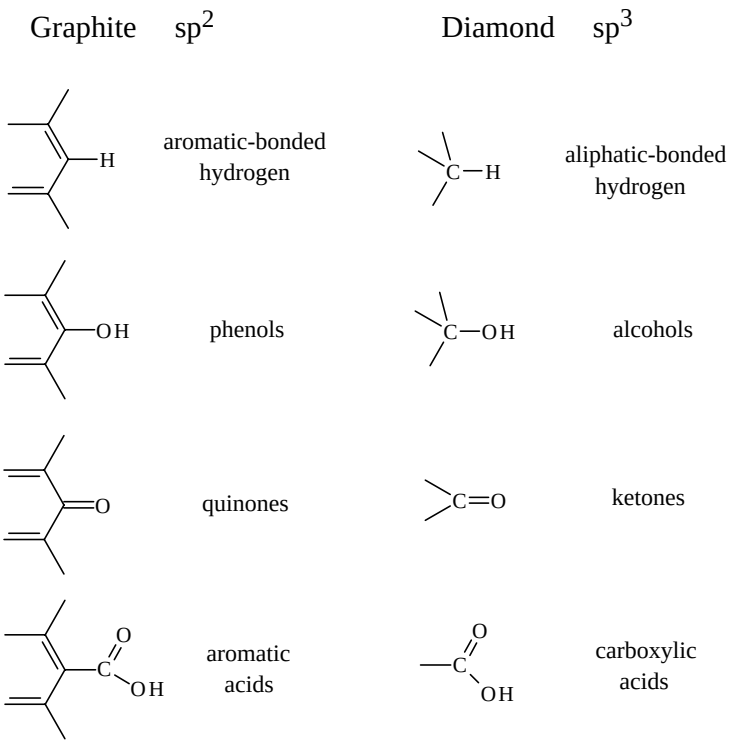

Fig. 5. Surface functional groups on oxidized sp^2 (graphite) and sp^3 (diamond) surfaces.

the aromatic functional groups and to the elimination of most of the sp^2 carbon from the surface (oxidation to CO_2). At the same time, the sp^2 carbon still present on the surface was activated [27]; in this case, a pair of peaks is seen (BDD_{mild} in inset in Figure 2) which probably is due to a hydroquinone/benzoquinone-like surface system [14, 24, 25]. A lower surface activity after stronger polarization (BDD_{severe}) could be explained in terms of a 'cleaner' polycrystalline diamond surface on which only less active aliphatic alcohol, ketone or carboxylic-like groups are present (Figure 5). The fact that the capacitance value for polished electrodes (BDD_{AcOH}) is similar to the frequency-dependent capacitance of a diamond single-crystal ($1\ \mu F\,cm^{-2}$) on which no species are supposed to be present [10, 28] supports the argument of a progressive elimination of the sp^2 species from the grain boundaries of diamond crystals by anodic oxidation.

The irreversibility of redox systems chosen as surface activity probes (ferri/ferrocyanide and 1,4-benzoquinone/hydroquinone) increased significantly between BDD_{ag} and BDD_{mild} (Tables 4 and 5). Values of the reaction rate constant, k° also were sensitive to surface oxidation. Elimination of non-diamond carbon (sp^2) species, as promoters of charge transfer reactions, is a likely explanation for the increase in irreversibility occurring with increasingly severe surface treatment.

A simple model could explain the behaviour of diamond electrodes [9]. The surface of diamond electrodes can be visualized as a diamond matrix in which sp^2 species are present. The reaction takes place on diamond as well as on the active sites offered by the sp^2. A distinct reaction rate constant can be associated with both processes; however, the reaction is faster on the sp^2 species than on diamond (Equation 5).

$$k_{sp^2} \gg k_{diamond} \tag{5}$$

5. Conclusion

The chemical and electrochemical properties of diamond electrodes were found to be strongly influenced by the surface treatment. A relatively mild polarization process was sufficient to transform the surface from hydrophobic (BDD_{ag}) to hydrophilic (BDD_{mild}) without changes in the crystal shape and size. The electrochemical properties were also strongly modified. The voltammetric charge decreased probably due to the decrease in the concentration of active surface sites. The calculated capacitance also decreased, which is typical for a surface partly depleted of functional groups. After stronger oxidation processes the electrodes had experienced morphological changes involving both crystal size and crystal shape (BDD_{severe} and BDD_{AcOH}). The surface became smoother, and the electrochemical activity measured in terms of voltammetric charge decreased strongly.

The irreversibility of redox systems chosen as surface activity probes (ferri/ferrocyanide and 1,4-benzoquinone/hydroquinone) increased significantly with surface treatment. The ΔE_p between the oxidation and reduction peaks increased. The transfer coefficients α_{red} and β_{ox} decreased, and their sum was lower than unity. Values of the reaction rate constant, k°, also were sensitive to surface oxidation. Anodic oxidation appears to result in a surface from which active species were eliminated.

The strong decrease in electrode activity following anodic treatment could be the result of a decrease in sp^2 as charge transfer promoters on the surface.

Acknowledgements

We thank the Swiss National Foundation for financial support for this project. We are grateful to the CSEM, Swiss Center for Electronics and Microtechnology, Neuchâtel hat for providing diamond electrodes and for financial support. Thanks also are due to the CIME, Interdepartmental Center of Electronic Microscopy at EPFL, Lausanne, and in particular to Mr Brian Senior and Prof. Philippe Buffat, for SEM measurements.

References

1. H.B. Martin, A. Argoitia, J.C. Angus and U. Landau, *J. Electrochem. Soc.* **146** (1999) 2959.
2. T. Kondo, Y. Einaga, B.V. Sarada, T.N. Rao, D.A. Tryk and A. Fujishima, *J. Electrochem. Soc.* **149** (2002) E179.
3. K. Hayashi, S. Yamanaka, H. Okushi and K. Kajimura, *Appl. Phys. Lett.* **68** (1996) 376.
4. I. Yagi, H. Notsu, T. Kondo, D.A. Tryk and A. Fujishima, *J. Electroanal. Chem.* **473** (1999) 173.
5. D.A. Tryk, K. Tsunozaki, T.N. Rao and A. Fujishima, *Diamond Relat. Mater.* **10** (2001) 1804.
6. R.J. Zhang, S.T. Lee and Y.W. Lam, *Diamond Relat. Mater.* **5** (1996) 1288.
7. C. Lévy-Clément, F. Zenia, N.A. Ndao and A. Deneuville, *New Diamond Front. Carbon Technol.* **9** (1999) 189.
8. G. M. Swain, A.B. Anderson and J.C. Angus, *MRS Bull.* **23** (1998) 56.
9. I. Duo, A. Fujishima and C. Comninellis, *Electrochem. Comm.* **5** (2003) 695.
10. M.C. Granger and G.M. Swain, *J. Electrochem. Soc.* **146** (1999) 4551.
11. H. Notsu, I. Yagi, T. Tatsuma, D.A. Tryk and A. Fujishima, *J. Electroanal. Chem.* **492** (2000) 31.
12. H. Notsu, I. Yagi, T. Tatsuma, D.A. Tryk and A. Fujishima, *Electrochem. and Solid State Lett.* **2** (1999) 522.
13. T.N. Rao and A. Fujishima, *Diamond Relat. Mater.* **9** (2000) 384.
14. D. Laser and M. Ariel, *J. Electroanal. Chem.* **52** (1974) 291.
15. A.J. Bard and L.R. Faulkner, 'Electrochemical Methods. Fundamentals and Applications' (J. Wiley & Sons, New York, 2001).
16. C.D. Hodgman, 'Handbook of Chemistry and Physics' (Chem. Rubber Publications, Cleveland, OH, 1944).
17. N.G. Ferreira, L.L.G. Silva, E.J. Corat and V.J. Trava-Airoldi, *Diamond Relat. Mater.* **11** (2002) 1523.
18. A.D. Modestov, Y.E. Evstefeeva, Y.V. Pleskov, V.M. Mazin, V. P. Varnin and I.G. Teremetskaya, *J. Electroanal. Chem.* **431** (1997) 211.
19. G. Kokkinidis, *J. Electroanal. Chem.* **172** (1984) 265.
20. M.N. Latto, D.J. Riley and P.W. May, *Diamond Relat. Mater.* **9** (2000) 1181.

21. H.J. Looi, L.Y.S. Pang, A.B. Molloy, F. Jones, J.S. Foord and R.B. Jackman, *Diamond Relat. Mater.* **7** (1998) 550.
22. J.v.d. Lagemaat, D. Vanmaekelbergh and J.J. Kelly, *J. Electroanal. Chem.* **475** (1999) 139.
23. G. Pastor-Moreno and D.J. Riley, *Electrochem. Comm.* **4** (2002) 218.
24. R.C. Engstrom and V.A. Strasser, *Anal. Chem.* **56** (1984) 136.
25. K.F. Blurton, *Electrochim. Acta* **18** (1973) 869.
26. P. Chen and R.L. McCreery, *Anal. Chem.* **68** (1996) 3958.
27. S. Alehashem, F. Chambers, J.W. Strojek, G.M. Swain and R. Ramesham, *Anal. Chem.* **67** (1995) 2812.
28. Y.V. Pleskov, Y.E. Evstefeeva, M.D. Krotova, V.Y. Mishuk, V.A. Laptev, Y.N. Palyanov and Y.M. Borzdov, *J. Electrochem. Soc.* **149** (2002) E260.